PHYSICAL REVIEW E, VOLUME 64, 051112

Self-generated disorder and structural glass formation in homopolymer globules

V. G. Rostiashvili,[1] G. Migliorini,[1] and T. A. Vilgis[1,2]
[1]Max Planck Institute for Polymer Research, 10 Ackermannweg, 55128 Mainz, Germany
[2]Laboratoire Européen Associé, Institute Charles Sadron, 6 Rue Boussingault, 67083 Strasbourg Cedex, France

(Received 30 May 2001; published 24 October 2001)

We have investigated the interrelation between spin glasses and structural glasses. Spin glasses in this case are p-spin interaction spin glasses (at $p>2$) or Potts glasses that contain quenched disorder, whereas the structural glasses are here exemplified by a homopolymeric globule, which can be viewed as a liquid of connected units on a nanoscale. It is argued that the homopolymeric globule problem can be mapped onto a disorder field theoretical model whose effective Hamiltonian resembles the corresponding one for the spin glass model. In this sense the disorder in the globule is self-generated (in contrast to spin glasses) and can be related to competing interactions (virial coefficients of different signs) and the chain connectivity. The work is aimed at giving a quantitative description of this analogy. We have investigated in the mean-field approximation the phase diagram of the homopolymeric globule where the transition line from the liquid to glassy globule is treated in terms of the replica symmetry breaking paradigm. The configurational entropy temperature dependence is also discussed.

DOI: 10.1103/PhysRevE.64.051112 PACS number(s): 05.40.−a, 36.20.−r, 75.10.Nr, 71.55.Jv

I. INTRODUCTION

The existing dynamical theory of glass-forming overcooled liquids and polymers is mainly applicable to the relatively high temperature area. The well-known mode-coupling theory (MCT) [1] predicts a dynamical phase transition at the critical temperature T_c where the overcooled liquid becomes nonergodic and stays in this state upon further cooling. It is significant that according to MCT the characteristic times of the α relaxation and the viscosity exhibit a power law divergence $\tau_\alpha(T) \propto \eta(T) \propto |T-T_c|^{-\gamma}$ at a critical temperature $T=T_c$. It is now realized that this type of singularity is generic for a broad class of mean-field (MF) models and its appearance is an indication of the role of *activation processes*, which are neglected in MF models [2]. This means physically that the topography of the free energy landscape in the space of the coarse grained variables should be taken into consideration. At low temperatures the free energy landscape determines more or less the dynamics of the system. The size of the free energy barriers between the metastable states, however, determines the rate of any activation processes in the low temperature regime $T<T_c$.

At the so-called Kauzmann temperature T_K, which is usually $T_K<T_c$, a genuine thermodynamic glass transition or so called Gibbs-DiMarzio transition is expected to take place [3]. At the Gibbs-DiMarzio (or Kauzmann) temperature T_K, the system is preferably in a thermodynamically unique configuration since the heights of the free energy barriers grow with increasing system size.

The earliest analytical approach to the problem that captured these two aforementioned aspects was worked out in several papers by Kirkpatrick, Thirumalai, and Wolynes in the late 1980s [4]. In these papers, which study the phenomena by making use of p-spin interaction spin glasses (at $p>2$) and Potts glasses with more than four components, the following conclusions were drawn.

(1) The predicted phase transition temperature T_A obtained by the dynamical theory (actually equivalent to T_c of the MCT based on Langevin dynamics in the mean-field limit) is higher than the Kauzmann T_K obtained by the static theory (or by the ordinary replica theory).

(2) As the temperature decreases (starting from the paramagnetic phase) the metastable minima appear first exactly at T_A.

(3) In the intermediate temperature regime $T_K<T<T_A$ many metastable states are separated by high barriers. In the mean-field limit these metastable states have an infinitely long lifetime. This is a well-known pathology of the MF model and a sharp transition does not occur in a finite dimensional system. Nevertheless, in a finite dimensional system T_A is physically significant, since for $T<T_A$ activated transport is the typical process.

(4) The overlap order parameter within the one-step replica symmetry breaking (1-RSB) scenario undergoes a discontinuous jump at T_K. This recalls a first order phase transition even though thermodynamically (e.g., in the specific heat) the transition seems to be of second order. The authors called this class of phase transitions *random first order phase transitions*. Crisanti and Sommers confirmed essentially the same type of behavior for the p-spin spherical model [5], which is different from the Sherrington-Kirkpatrick [6] model, and the behavior is shared by some other spin glass models [7].

Indeed, it has been argued often that many connections exist between the behavior of structural glasses and spin glasses without reflection symmetry [2,4,7]. Most of the properties mentioned above for the spin glass can be found in the context of structural glasses too. However, the important difference between the spin and structural glasses is that the spin glasses models already contain a quenched disorder in the Hamiltonian. In structural glasses the Hamiltonian is a regular function of the particle coordinates and does not contain disorder. Nevertheless, the free energies in both systems resemble each other and possess similar properties. Thus, the disorder is in a sense self-generated and develops during the cooling (or glass transition) process.

The properties and possibilities of self-generated (or self-

1063-651X/2001/64(5)/051112(16)/$20.00

induced) disorder have already been discussed in the framework of rather special spin models [2,8]. These models explicitly involve pseudorandom numbers, i.e., the spin-spin couplings, although deterministic, oscillate very rapid and can be considered as (pseudo)random variables. These models, however, provide some spin analogies with structural glasses but still are quite different from structural glasses [2].

Furthermore, the ideas and the methods of the mean-field spin glass models [9–11] have been successfully used to study the freezing states in a heteropolymer globule [12–15]. The corresponding model considers the conformational behavior of a polymer chain with randomly quenched interactions between monomers. These random copolymers always possess a collapsed (or globular state) depending on the temperature and the strength of the randomness. It was successfully shown that the disorder results in a globular and eventually in a glassy globular state. The corresponding freezing is characterized by a transition between two phases: one phase is characterized by many accessible configurations, while the other is dominated by only a few of them, i.e., an eventually frozen state. In this context heteropolymer freezing usually serves as a simple ''toy model'' for the protein folding phenomenon [15]. This relationship between the freezing and folding phenomena is caused mainly by the fact that in both cases only a single conformation (which in the context of protein folding is called the native state) dominates.

In the following we are going to investigate a similar problem in homopolymer globules in poor solvent. It is well known that homopolymers in poor solvent form globules due to an attractive second virial coefficient; the globules are then stabilized by the repulsive third virial coefficient [16]. The relevant parameter for globule formation is the second virial coefficient which is measured by the relative distance from the so-called Θ temperature, where the homopolymer takes Gaussian conformations. Just below Θ the polymer collapses and the lower the temperature the more dense becomes the globule. The intuitive limit is then a dense liquid globule. We will show, nevertheless, that even at lower temperatures and beyond a certain density the globule freezes and forms a glass. Homopolymer globules show a structural glass transition. Thus the system will form a ''nanoglass,'' i.e., a frozen and condensed polymer chain restricted to the scale of the individual globule.

It is most interesting to note that in recent Monte Carlo simulations of homopolymer globules, Milchev and Binder [17] found a dramatic decrease of the acceptance rate of the moves, which in its turn suggests the growth of the characteristic times. They saw also pronounced density fluctuations which appear in the center of the globule and spread over the entire globule as the temperature is lowered. These results were interpreted in terms of a glassy type of transition. These investigations have been restudied in papers by Kreitmeier *et al.* [18–20] where a similar dynamical behavior of the homopolymer globule was verified once more and generalized for the cyclic deformation regime. Moreover, the glass transition in a homopolymer globule (for chain length $N<27$ on a $3\times3\times3$ cubic lattice) was investigated by computer simulations [21]. These authors found that the conformation space of the model consisted of one huge valley and a large number of small ''chambers.'' These disjoint domains of the conformational space are responsible for the ergodicity breaking and freezing transition. This might be important for the final processes of folding dynamics in protein molecules because the speed and reliability of the folding depends on whether the native state belongs to the same conformational space domain or not [15].

The thermodynamic behavior of homopolymer globules has been studied also by discontinuous molecular dynamics simulation [22,23]. By making use of a simple off-lattice model for chain length $N=64$ the authors showed the existence of a first order liquid-solid-like transition. The transition occured at temperatures below the coil-globule transition temperature and was detected by a heat capacity peak as well as by a Lindemann parameter jump. It is interesting that there is a qualitative similarity between homopolymers and proteins where the transition from the molten globule to the native state is also of first order [24,25]. In Ref. [26] an ''expanded ensemble'' Monte Carlo algorithm was introduced which helps to overcome the density slowing down in the globule state. For chain lengths up to $N=512$ the authors saw a bimodal distribution in the number of contacts per monomer. This is again a clear indication of a first order liquid-to-solid transition of the collapsed globule.

As already mentioned, it is most important that the globule formed from ordinary homopolymers does not contain any quenched disorder. If this system forms glassy states the disorder has to be self-generated. Nevertheless, to form glassy states certain frustrations are necessary. These may result from the interplay between attractive interaction (negative second virial coefficient v), repulsion (positive third virial coefficient w), and the constraints imposed by the chain connectivity. These frustrations might already be sufficient to provide a structural glass transition from a liquid globule to a glassy globule.

The main purpose of the present paper is to investigate these problems in more detail by analytical means. We will indeed show that a linear homopolymer in the condensed globular phase undergoes a genuine structural glass transition of a type similar to that in a p-spin interaction spin glass with $p>2$ or a Potts glass model. We stress once more that the homopolymer is a pure system and does not contain quenched disorder. Nevertheless, the n-component field theory formulation for linear polymers [27] already provides a natural and solid basis [28]. As we will show below, the homopolymer globule is a generic system where frustrations rather than quenched disorder trigger the glass formation. As a starting point we employ the field-theoretical description of a self-interacting polymeric chain in a poor solvent [29,30]. So far, in Refs. [29,30] it has been shown that the Laplace transformation (with respect to the chain length N) of the polymeric correlation function can be associated with the corresponding correlator within the $n\rightarrow0$ limit of the n-component ψ_a^4,ψ_a^6 field theory (where $a=1,\ldots,n$). We argue instead that the same n-component field theory can be mapped onto some kind of disordered one-component model where the imposed random field is non-Gaussian (colored noise) and its statistical moments are determined only by virial coefficients $v, w, \ldots$, etc. In this case the index a acts as a replica index for spin glasses [9,10] or random magnetics [11]. This mapping has already been suggested for spin glasses three decades ago [31,32] but was never actually used. At this point we should add a general remark. Throughout the paper we use the large globule approximation, i.e., we consider the chain length N to be very large. This is necessary to avoid additional complications close to the surface of the globule. Intuitively it is obvious that monomers close to the globule surface experience a different dynamic environment, such that different mechanisms of freezing take place. We will come back to this point in a later publication.

II. THE HOMOPOLYMER GLOBULE AS A DISORDERED SYSTEM

A. The field theory representation

In this section we will provide the basic formulations and the field theory for polymers in poor solvent, i.e., with attractive interactions caused by a negative second virial coefficient. To do so, we start from the usual continuous description of a homopolymer chain of length N in a poor solvent. The chain conformation is characterized by the d-dimensional vector function $\mathbf{r}(s)$, where s $(0 \leqslant s \leqslant N)$ enumerates segments of the chain. The corresponding Edwards Hamiltonian has the following form [30]:

$$H[\mathbf{r}(s)] = \frac{d}{2a^2}\int_0^N ds\left(\frac{\partial \mathbf{r}(s)}{\partial s}\right)^2 - \frac{|v|}{2}\int_0^N ds ds'\, \delta(\mathbf{r}(s) - \mathbf{r}(s')) + \frac{w}{3!}\int_0^N ds ds' ds''\, \delta(\mathbf{r}(s)-\mathbf{r}(s'))\delta(\mathbf{r}(s') - \mathbf{r}(s'')). \tag{2.1}$$

The first term in the Hamiltonian (2.1) is responsible for the chain connectivity, whereas the two other terms are connected with the virial expansion. In Eq. (2.1) we already imposed the condition that the second virial coefficient is negative, $v<0$, and the third virial coefficient $w>0$. Usually the second virial coefficient is measured by its distance from the Θ temperature, i.e., $|v| \simeq a^3 |T-\Theta|/\Theta = a^3\tau$. The third virial coefficient is always of the order of $w \sim O(a^6)$. The density of the globule is easily estimated by $\rho \simeq |v|/w$, which provides a naive limit of the temperature at $\rho a^3 = 1$. Indeed, at sufficient low temperatures the globule is dense, and the entropy term (first term) becomes less and less important. The remaining entropic fluctuations are important only on length scales $\xi \simeq a/\tau$. This observation will allow us later the safe use of corresponding mean-field theories.

The next step [29,30,33] (see also Appendix A) is to employ the Laplace transformation of the polymeric correlation function $\Xi(\mathbf{r}_1, \mathbf{r}_2; N)$,

$$\Xi(\mathbf{r}_1, \mathbf{r}_2; \mu) = \int_0^\infty dN\, \Xi(\mathbf{r}_1, \mathbf{r}_2; N)\exp(-\mu N), \tag{2.2}$$

which can be associated with the $n \to 0$ limit of the ψ_a^4, ψ_a^6 field theory as follows:

$$\Xi(\mathbf{r}_1, \mathbf{r}_2; \mu) = \lim_{n\to 0}\int \prod_{a=1}^{n} D\psi_a \psi_1(\mathbf{r}_1)\psi_1(\mathbf{r}_2) \times \exp\{-H_n[\vec{\psi}; \mu]\}, \tag{2.3}$$

where $\vec{\psi} = \{\psi_1, \psi_2, \ldots, \psi_n\}$ is an n-component field and μ the chemical potential, which is conjugate to N, and the replicated Hamiltonian is

$$H_n[\vec{\psi}; \mu] = \frac{1}{2}\int d^d r \sum_{a=1}^{n} \psi_a(\mathbf{r})\left[\mu - \frac{a^2}{2d}\nabla^2\right]\psi_a(\mathbf{r}) - \frac{|v|}{8}\int d^d r\left[\sum_{a=1}^{n}\psi_a^2(\mathbf{r})\right]^2 + \frac{w}{3!8}\int d^d r\left[\sum_{\alpha=1}^{n}\psi_a^2(\mathbf{r})\right]^3 + \cdots. \tag{2.4}$$

As usual the vector field ψ corresponds to the polymer density in the usual manner, i.e., $\rho \propto \langle \psi_1^2 \rangle$. The relationship between μ and N has the form

$$N = -\frac{(\partial/\partial\mu)\int d^d r_1 d^d r_2 \Xi(\mathbf{r}_1, \mathbf{r}_2; \mu)}{\int d^d r_1 d^d r_2 \Xi(\mathbf{r}_1, \mathbf{r}_2; \mu)}. \tag{2.5}$$

The attractive interaction term of order ψ^4 changes the behavior of the field theory. Correlations of the self-avoidance are no longer important and we must consider the balance between the attractive and repulsive forces. Although we mentioned above the relative unimportance of the connectivity term, we have to keep track of it as well. The careful analysis below shows that it provides at sufficiently low second virial coefficients significant contributions on small scales $[\xi \sim O(a)]$ that are caused only by connectivity. These are in part responsible for frustration.

B. Mapping onto a random model

Now we are going to map this field theory onto a random system. It can be shown (see Appendix B) that the free energy of the globule state F_{Gl} can be interpreted as the free energy of a one-component random model with Hamiltonian

$$\mathcal{H}\{\psi\} = \frac{1}{2}\int d^d r\left[\mu\psi^2(\mathbf{r}) + \frac{a^2}{2d}(\boldsymbol{\nabla}\psi)^2 + t(\mathbf{r})\psi^2(\mathbf{r})\right], \tag{2.6}$$

where the random field $t(\mathbf{r})$ is non-Gaussian with its generating functional of the form

$$\Phi\{\rho(\mathbf{r})\} \equiv \overline{\exp\left\{-\int d^d r\, t(\mathbf{r})\rho(\mathbf{r})\right\}} = \exp\left\{\frac{|v|}{8}\int d^d r\, \rho^2(\mathbf{r}) - \frac{w}{3!8}\int d^d r\, \rho^3(\mathbf{r})\right\}, \tag{2.7}$$

and where the overbar means averaging over $t(\mathbf{r})$. It is interesting to underline that only for this combination of signs of the virial coefficients $(v<0, w>0)$ are the even central moments $\overline{t(r_1)t(r_2)\cdots t(r_{2m})}$ [see Eqs. (B8)–(B11)] positive, as they should be for a real field $t(\mathbf{r})$. The aforementioned mapping takes the form

$$F_{\mathrm{Gl}} = -\lim_{n\to 0}\frac{1}{n}\ln \overline{Z^n}, \tag{2.8}$$

where the replicated partition function is

$$\overline{Z^n} = \int D\vec{\psi}\exp\{-H_n\}. \tag{2.9}$$

In the present paper we are going to use this analogy between the homopolymer model (which is a ''pure'' model, i.e., does not include quenched disorder in its Hamiltonian) and the random model (2.6).

C. Legendre transformation

As a next step we should go to the two-replica variables $Q_{ab}(\mathbf{r})$, or Parisi overlaps [9] for polymers [28]. One can implement this using the Legendre transformation of the interaction part of the Hamiltonian (2.4) which can be represented in the form

$$K[u_{ab}] \equiv \frac{|v|}{8}\int d^d r \sum_{a,b=1}^{n} u_{ab}u_{ba} - \frac{w}{3!8}\int d^d r \sum_{a,b=1}^{n} u_{ab}u_{bc}u_{ca} - \frac{z}{4!16}\int d^d r \sum_{a,b=1}^{n} u_{ab}u_{bc}u_{cd}u_{da} + O(u_{ab}^5), \tag{2.10}$$

where the pair field $u_{ab}(\mathbf{r}) \equiv \psi_a(\mathbf{r})\psi_b(\mathbf{r})$ and where we have also kept the fourth virial coefficient z. Let us introduce the integral transformation

$$\exp\{K[u_{ab}]\} = \int \prod_{c,d}^{n} DQ_{cd}(\mathbf{r})\exp\left\{W[Q_{ab}] + \int d^d r \sum_{a,b}^{n} Q_{ab}(\mathbf{r})u_{ab}(\mathbf{r})\right\} \tag{2.11}$$

and find $W[Q_{ab}]$ in the form of a functional expansion. For this purpose one should use the saddle point method in Eq. (2.11) which can be carried out in the same spirit as in Refs. [34,35]. This results in the Legendre transformation with respect to the extremum field $\overline{Q}_{ab}$,

$$K[u_{ab}(\mathbf{r})] = W[\overline{Q}_{ab}(\mathbf{r})] + \int d^d r \sum_{a,b=1}^{n} \overline{Q}_{ab}(\mathbf{r})u_{ab}(\mathbf{r}). \tag{2.12}$$

As a result [36] we get

$$\frac{\delta K}{\delta u_{ab}} = \overline{Q}_{ab}(\mathbf{r}), \tag{2.13}$$

$$\frac{\delta W}{\delta \overline{Q}_{cd}(\mathbf{r})} = -u_{cd}. \tag{2.14}$$

By making use of the expansion (2.10) in Eqs. (2.13) and (2.14) one obtains for $W[Q_{ab}]$ the following expression:

$$W[Q_{\alpha\beta}(\mathbf{r})] = -\frac{2}{|v|}\int d^d r\, \mathrm{Tr}(Q^2) - \frac{4w}{3|v|^3}\int d^d r\, \mathrm{Tr}(Q^3) - \frac{2}{|v|^4}\left(\frac{w^2}{|v|}+\frac{z}{3}\right)\int d^d r\, \mathrm{Tr}(Q^4) + O(Q^5). \tag{2.15}$$

After the transformation (2.11) the replicated partition function (2.9) takes the form

$$\overline{Z^n} = \int \prod_{c,d}^{n} DQ_{cd}(\mathbf{r})\exp\left\{-\frac{1}{2}\mathrm{Tr}\ln\left\{\left[\mu - \frac{a^2}{2d}\nabla^2\right]\delta_{ab} - 2Q_{ab}(\mathbf{r})\right\} + W[Q_{ab}(\mathbf{r})]\right\}. \tag{2.16}$$

So far only mathematical identities have been used. Nevertheless, the use of the overlap variables Q_{ab} allows us to detect completely different correlations from the classical $O(n)$ field theory in the limit $n\to 0$ for self-avoiding walks. They will allow us to probe for a more complicated phase space and provide information on the presence of glassy-type correlations in the globules. With this in mind it appears instructive to express the generalization of the polymeric correlation function (2.3)

$$\Xi_{ab}(\mathbf{r}_1,\mathbf{r}_2;\mu) = \langle \psi_a(\mathbf{r}_1)\psi_b(\mathbf{r}_2)\rangle \tag{2.17}$$

in terms of overlaps $Q_{ab}(\mathbf{r})$. To this end we add the source term $\psi_a(\mathbf{r})h_a(\mathbf{r})$ in Eq. (2.11). After substitution in Eq. (2.9) and integration over $\vec{\psi}$ one gets

$$\Xi_{ab}(\mathbf{r},\mathbf{r}';\mu) = \langle\{[\hat{1}\cdot G_0^{-1} - 2\hat{Q}]^{-1}\}_{ab}\rangle(\mathbf{r},\mathbf{r}'), \tag{2.18}$$

where $G_0^{-1} = \mu - (a^2/2d)\nabla^2$. The corresponding polymer correlator (2.3) is nothing but the $\Xi_{11}(\mathbf{r},\mathbf{r}';\mu)$ element of the matrix (2.18).

The correlator $\Xi_{ab}(\mathbf{r},\mathbf{r}';\mu)$ measures the probability of finding a chain configuration starting at $\mathbf{r}$ in the replica a provided that it ends at $\mathbf{r}'$ in the replica b. From Eq. (2.18) this correlator can also be seen as the scattering amplitude of a free ‘‘particle’’ with the Green function G_0 on the ‘‘scatterers’’ whose density is described by Q_{cd}.

The present representation (2.16) is very promising and recalls the corresponding expressions for spin glass models [3,5,9,10]. The striking difference between these two cases is that in Eq. (2.16) only the pure model parameters (Kuhn's segment length and virial coefficients) are involved. As a result the representation can provide a good starting point for the phenomenon of self-generated disorder which, as we believe, is behind the structural glass formation.

III. MEAN-FIELD TREATMENT

A. Landau-type expansion

In order to simplify the mean-field treatment of the integral (2.16) let us expand the effective Hamiltonian in Eq. (2.16) to fourth order. We obtain by this procedure

$$\begin{aligned}\overline{Z^n}=&\int\prod_{a,b=1}^{n}DQ_{ab}(\mathbf{r})\\&\times\exp\Bigg\{-\sum_{a,b=1}^{n}\int d^dr_1d^dr_2\Gamma^{(2)}(\mathbf{r}_1,\mathbf{r}_2)Q_{ab}(\mathbf{r}_1)Q_{ba}(\mathbf{r}_2)\\&-\sum_{a,b,c=1}^{n}\int d^dr_1d^dr_2d^dr_3\Gamma^{(3)}(\mathbf{r}_1,\mathbf{r}_2,\mathbf{r}_3)Q_{ab}(\mathbf{r}_1)\\&\times Q_{bc}(\mathbf{r}_2)Q_{ca}(\mathbf{r}_3)-\sum_{a,b,c,d=1}^{n}\int d^dr_1d^dr_2d^dr_3d^dr_4\\&\times\Gamma^{(4)}(\mathbf{r}_1,\mathbf{r}_2,\mathbf{r}_3,\mathbf{r}_4)Q_{ab}(\mathbf{r}_1)Q_{bc}(\mathbf{r}_2)Q_{cd}(\mathbf{r}_3)Q_{da}(\mathbf{r}_4)\Bigg\},\end{aligned}\tag{3.1}$$

where the coefficients

$$\Gamma^{(2)}(\mathbf{r}_1,\mathbf{r}_2)=\frac{2}{|v|}\delta(\mathbf{r}_1-\mathbf{r}_2)-G_0(\mathbf{r}_1-\mathbf{r}_2)G_0(\mathbf{r}_2-\mathbf{r}_1),$$

$$\begin{aligned}\Gamma^{(3)}(\mathbf{r}_1,\mathbf{r}_2,\mathbf{r}_3)=&\frac{4}{3}\Bigg[\frac{w}{|v|^3}\delta(\mathbf{r}_1-\mathbf{r}_2)\delta(\mathbf{r}_2-\mathbf{r}_3)\\&-G_0(\mathbf{r}_1-\mathbf{r}_2)G_0(\mathbf{r}_2-\mathbf{r}_3)G_0(\mathbf{r}_3-\mathbf{r}_1)\Bigg],\end{aligned}$$

$$\begin{aligned}\Gamma^{(4)}(\mathbf{r}_1,\mathbf{r}_2,\mathbf{r}_3,\mathbf{r}_4)=&\frac{2}{|v|^4}\left(\frac{w^2}{|v|}+\frac{z}{3}\right)\delta(\mathbf{r}_1-\mathbf{r}_2)\delta(\mathbf{r}_2-\mathbf{r}_3)\\&\times\delta(\mathbf{r}_3-\mathbf{r}_4)-G_0(\mathbf{r}_1-\mathbf{r}_2)G_0(\mathbf{r}_2-\mathbf{r}_3)\\&\times G_0(\mathbf{r}_3-\mathbf{r}_4)G_0(\mathbf{r}_4-\mathbf{r}_1).\end{aligned}\tag{3.2}$$

As often in MF theories the order parameter Q_{ab} does not depend on the spatial coordinate $\mathbf{r}$. As is customary in the MF theory of the spin glass models [9–11], we decompose the Parisi matrix Q_{ab} in the following form:

$$Q_{ab}=(q-f)\delta_{ab}+f+\Delta_{ab}.\tag{3.3}$$

In Eq. (3.3) the symmetric part $R_{ab}=(q-f)\delta_{ab}+f$, with the diagonal q and off-diagonal f elements, describes the replica symmetric (RS) solution [9–11]. The matrix Δ_{ab} equals zero for $a=b$ and is responsible for the replica symmetry breaking (RSB) [9–11]. The use of the decomposition (3.3) in Eq. (3.1) allows one in the MF approximation to separate the total free energy into RS and RSB parts. During the calculation of the traces in Eq. (3.1) it is convenient to use Parisi's representation of Δ_{ab} by a function $\Delta(x)$, where $0\leqslant x\leqslant 1$. Then the free energy is found to be

$$\lim_{n\to 0}\frac{1}{nV}F\{Q_{ab}\}=f_{\mathrm{RS}}\{q,f\}+f_{\mathrm{RSB}}\{q,f;\Delta(x)\},\tag{3.4}$$

where the RS free energy

$$\begin{aligned}f_{\mathrm{RS}}\{q,f\}=&A(q^2-f^2)+B(q^3-3qf^2+2f^3)\\&+C(q^4-6q^2f^2+8qf^3-3f^4)\end{aligned}\tag{3.5}$$

and the RSB free energy

$$\begin{aligned}f_{\mathrm{RSB}}\{q,f;\Delta(x)\}=&-w_1\int_0^1dx\Delta^2(x)-w_2\left[\int_0^1dx\Delta(x)\right]^2-w_3\int_0^1dx\left[x\Delta^3(x)+3\Delta(x)\int_0^xdy\Delta^2(y)\right]+w_4\left[\int_0^1dx\Delta(x)\right]^3\\&+w_5\Bigg\{4\int_0^1dx\Delta(x)\int_0^xdyy\Delta^3(y)+\int_0^1dxx^2\Delta^4(x)+2\int_0^1dx\Delta^2(x)\Bigg(\left[\int_0^1dy\Delta(y)\right]^2+2\left[\int_x^1dy\Delta(y)\right]^2\\&-2\int_0^xdy\Delta(y)\int_y^1dz\Delta(z)\Bigg)\Bigg\}\end{aligned}\tag{3.6}$$

The coefficients in Eqs. (3.5) and (3.6) are given in Appendix C by Eqs. (C10)–(C17).

The minimization of f_{RS} leads to the RS solution, q_m and f_m, whereas the maximization (as is the case for spin glasses [9–11]) of f_{RSB} results in the RSB solution in terms of the overlap matrix $\Delta(x)$. The coefficients in the Landau expansion of f_{RSB} depend also on the RS solution.

In order to take into account the spatial correlation in the

RS sector (see Sec. V B), it is convenient to assume that the variable q and the coefficients A,B, and C are weakly $\mathbf{k}$ dependent. In this case the Landau expansion is more involved and is given in Appendix C.

B. Density in terms of Q_{ab}

The essential issue is to express the globule density ρ in terms of the order parameter Q_{ab}. This allows one to detect any glassy features inside the globule and to distinguish between the liquid and glassy phases. Moreover, it will show any unusual properties of the phase space. As mentioned already in the introductory remarks the density is determined by the ψ fields. In the MF approximation the local monomer density is given in terms of the grand canonical partition function as

$$\rho(\mathbf{r})=\int_0^N ds\,\frac{\int d^dr\,\Xi(\mathbf{r};s)\Xi(\mathbf{r}-\mathbf{r}';N-s)}{\int d^dr\,\Xi(\mathbf{r};N)},\tag{3.7}$$

which should be supplemented by the normalization condition (mass conservation), i.e.,

$$\int d^dr\,\rho(\mathbf{r})=N.\tag{3.8}$$

By making use of Eqs. (3.7) and (3.8) and after Laplace transformation we find

$$\int d^dr\int d^dr'\,\Xi(\mathbf{r}';\mu)\Xi(\mathbf{r}-\mathbf{r}';\mu)=-\frac{\partial}{\partial\mu}\int d^dr\,\Xi(\mathbf{r};\mu),\tag{3.9}$$

where $\Xi(\mathbf{r};\mu)$ is the Laplace transformation of $\Xi(\mathbf{r};N)$ [see Eq. (2.2)]. Then the equation that determines the chain length becomes

$$N=-\frac{\partial}{\partial\mu}\ln\left\{\int d^dr\,\Xi(\mathbf{r};\mu)\right\}\tag{3.10}$$

and takes the form

$$N=\frac{\int d^dr\int d^dr'\,\Xi(\mathbf{r}';\mu)\Xi(\mathbf{r}-\mathbf{r}';\mu)}{\int d^dr\,\Xi(\mathbf{r};N)}.\tag{3.11}$$

In the MF approximation Eq. (2.3) reads

$$\Xi(\mathbf{r})=\psi_1^{\mathrm{mf}}(\mathbf{r})\psi_1^{\mathrm{mf}}(0),\tag{3.12}$$

where $\psi_1^{\mathrm{mf}}(\mathbf{r})$ is the MF solution for $\psi_1(\mathbf{r})$. Combining Eqs. (3.12) with (3.11) and (3.8) leads to the expected result

$$\rho(\mathbf{r})=[\psi_1^{\mathrm{mf}}(\mathbf{r})]^2.\tag{3.13}$$

Finally, in order to express the density in terms of Q_{ab} we recall that the pair field $u_{11}^{\mathrm{mf}}=[\psi_1^{\mathrm{mf}}(\mathbf{r})]^2$ (see Sec. II C). Combining this with Eqs. (2.14) and (2.15) and taking into account the decomposition (3.3) one obtains the following expansion for the density:

$$\begin{aligned}\rho=&\frac{4}{|v|}q+\frac{4w}{|v|^3}q^2+\frac{8}{|v|^4}\left(\frac{w^2}{|v|}+\frac{z}{3}\right)q^3+\frac{4w}{|v|^3}\left[-\int_0^1 dx\,\Delta^2(x)\right]\\&+\frac{8}{|v|^4}\left(\frac{w^2}{|v|}+\frac{z}{3}\right)\left[-3q\int_0^1 dx\,\Delta^2(x)+\int_0^1 dx\left(x\Delta^3(x)\right.\right.\\&\left.\left.+3\Delta(x)\int_0^x dy\,\Delta^2(y)\right)\right].\end{aligned}\tag{3.14}$$

In Eq. (3.14) we have used Parisi's representation of Δ_{ab} and taken into account that the off-diagonal element vanishes, $f=0$ (see below). The "singularity" $|v|\rightarrow 0$ in Eq. (3.14) is spurious, as we will see in the next section. In the MF approximation the value of q becomes $|v|$ dependent itself, i.e., $q\propto|v|^2$ and $\Delta(x)\propto|v|^2$, so that $\rho\rightarrow 0$ at $v\rightarrow 0$, as it should close to the Θ temperature.

IV. Θ POINT REGIME: COIL-GLOBULE TRANSITION

The question that must be resolved first is the ordinary coil-globule transition. In any case the present general approach should reproduce the physical properties of the standard coil-globule transition [27,37]. We investigate the system just below the Θ temperature $T<\Theta$. In Refs. [29,30] the standard O(n) field-theoretic formulation (see Sec. II A) was used in order to treat this problem beyond scaling. The method of pair fields, which is a simpler version of the present formulation [38], was developed and applied to the coil-globule transition. In that earlier paper of one of the present authors the third virial coefficient was not taken into account, which corresponds to an expansion around the Θ point regime. Here, the Legendre transformation method from Sec. II C makes it easy to take into account an arbitrary number of virial coefficients.

In the Θ point region (i.e., at $T\leqslant\Theta$) the globule conformations are very close to Gaussian forms so that for the chemical potential one can expect the scaling $\mu=\mu_0/N$. In this case it is convenient to rescale the virial coefficients $|v|,w$, and z in the following way:

$$x=\frac{|v|}{a^d}N^{(4-d)/2},\tag{4.1}$$

$$y=\frac{w}{a^{2d}}N^{3-d},\tag{4.2}$$

$$t=\frac{z}{a^{3d}}N^{(8-3d)/2},\tag{4.3}$$

which shows the upper critical dimensions of the different terms in the virial expansion. After that the scaling forms of the coefficients (C10), (C11), and (C12) are given by

$$A=\frac{N^{(4-d)/2}}{a^{d}}\left[\frac{2}{x}-\left(\frac{d}{2\pi}\right)^{d/2}\frac{\Gamma((4-d)/2)}{\mu_0^{(4-d)/2}}\right], \qquad (4.4)$$

$$B=\frac{4\,N^{(6-d)/2}}{3\,a^{2d}}\left[\frac{y}{x^{3}}-\left(\frac{d}{2\pi}\right)^{d/2}\frac{\Gamma((6-d)/2)}{2\,\mu_0^{(6-d)/2}}\right], \qquad (4.5)$$

$$C=\frac{N^{(8-d)/2}}{a^{3d}}\left[2\,\frac{y^{2}}{x^{5}}+\frac{2}{3}\,\frac{t}{x^{4}}-\left(\frac{d}{2\pi}\right)^{d/2}\frac{\Gamma((8-d)/2)}{3\,\mu_0^{(8-d)/2}}\right]. \qquad (4.6)$$

In the Θ point regime $|v|=a^{d}(1-T/\Theta)\to 0$ and $N\gg 1$, so that at $d=3$ $x\approx 1$, $y\approx 1$, and $t\ll 1$, i.e., the fourth virial coefficient becomes irrelevant.

In the present regime only the RS solution makes physical sense, since no other solution than the onset of the liquid globule can be expected. Thus we minimize the RS free energy (3.5) with respect to q and f. The resulting solution reads

$$f_m=0, \qquad (4.7)$$

$$q_m=\frac{-3B+\sqrt{(3B)^{2}+32|A|C}}{8C}, \qquad (4.8)$$

so that the RS free energy becomes

$$f_{\rm RS}\{q\}=A\,q^{2}+B\,q^{3}+C\,q^{4}. \qquad (4.9)$$

Let us consider a possible second order phase transition and impose the conditions: $A\leqslant 0, B>0$, and $C>0$. In the vicinity of the transition point the coefficient A becomes small, $|A|\ll 1$, and the order parameter takes the value

$$q_m\approx\frac{2\,|A|}{3\,B}. \qquad (4.10)$$

As is seen from Eqs. (4.4) and (4.5), in $d=3$ the order parameter scales as $q_m\propto 1/N$. Thus, it follows from Eq. (3.14) that the density scales as $\rho=4q_m/|v|$, which means physically $\rho=1/N^{1/2}$ (note also that $x\approx 1$ and $|v|\propto N^{-1/2}$). Therefore we reproduce the correct scaling for the density, which is found also from naive scaling.

We can also obtain the transition line in the $|v|$-w plane, which will be the first step toward a more general phase diagram spanned by the virial coefficients. This line is defined by the conditions $A=0, B>0$, and $C>0$, which again for three dimensions $d=3$ yield

$$\mu_0=\left(\frac{x}{2}\right)^{2}\left(\frac{3}{2\pi}\right)^{3}\left[\Gamma\left(\frac{1}{2}\right)\right]^{2}, \qquad (4.11)$$

$$\frac{y}{x^{3}}>\left(\frac{3}{2\pi}\right)^{3/2}\frac{\Gamma\left(\frac{3}{2}\right)}{2\,\mu_0^{3/2}}, \qquad (4.12)$$

$$\frac{y^{2}}{x^{5}}>\left(\frac{3}{2\pi}\right)^{3/2}\frac{\Gamma\left(\frac{5}{2}\right)}{6\,\mu_0^{3/2}}. \qquad (4.13)$$

It is interesting that if Eq. (4.11) is valid then conditions (4.12) and (4.13) merge and convert into the globule stability condition $y>16\pi^{2}/27$. We can eliminate μ_0 in Eq. (4.11) by combining Eq. (3.10) with the polymer correlation function

$$\Xi(\mathbf{k};\mu)=\frac{1}{(a^{2}/6)k^{2}+\mu-2q_m}. \qquad (4.14)$$

We recall that in Eq. (4.14) $\mu=\mu_0/N$ and $q_m=q_m^{0}/N$. The result of the combining reads

$$\mu_0=1+2q_m^{0}-2\,\frac{\partial}{\partial\mu_0}q_m^{0}. \qquad (4.15)$$

By making use of Eqs. (4.10) and (4.11) in Eq. (4.15) for the transition line, one gets

$$\left(\frac{x}{2}\right)^{2}\left(\frac{3}{2\pi}\right)^{3}=1+\left(\frac{4}{3}\right)\frac{\frac{16}{27}\pi^{2}}{y-\frac{16}{27}\pi^{2}}, \qquad (4.16)$$

where the globule stability condition $y>16\pi^{2}/27$ is implied.

For completeness we check for the possibility of a first order phase transition. The necessary conditions for this are $A>0, B<0$, and $C>0$ [see Eq. (4.9)]. It is simple to see from Eqs. (4.4)–(4.6) that these conditions are contradictory. This means that within our MF approach only the second order coil-globule phase transition is possible, which is in accordance with the well-known result [37]. Therefore the present field-theoretic formulation is able to reproduce the standard coil-globule transition as the replica symmetric solution at conditions close to the Θ temperature.

V. DEEPER IN THE GLOBULE STATE: LIQUID VERSUS GLASSY REGIME

A. RSB solution in the globule

In this section we investigate the possibility of replica broken solutions deeper in the globular state. The globule density from naive scaling is given by $\rho a^{3}=a^{3}|v|/w=\tau$ and has a natural limit at $\tau=1$. Physically this limit corresponds to a dense globular state without any solvent inside. At temperatures below the coil-globule phase transition, but still far above $\tau=1$, the system is usually characterized by a monomer-monomer correlation length $\xi<R_{\rm Gl}\propto N^{1/3}$. In this case the chemical potential and the density are no longer N dependent. It can be seen from dimensional analysis and simple scaling arguments [27,30,37] that the chemical potential scales as $\mu\propto|v|^{2}/w\propto\tau^{2}$, the density $\rho_{\rm Gl}\propto|v|/w\propto\tau$, and $\xi\propto 1/|v|\propto\tau^{-1}$.

In this regime fluctuations can still be important unless $a\ll\xi\ll R_{\rm Gl}$, where the MF solution, which we discussed in Sec. III, becomes valid. Here one can expect that, because of competing interactions (negative second virial coefficient versus positive third virial coefficient) and the constraints imposed by the chain connectivity, only a few conformations will dominate. This could manifest itself as the glass transition long known for spin glass models [9–11] and heteropolymers [15]. Formally speaking, this transition shows itself as a nontrivial solution that maximizes the RSB free energy functional (3.6).

Before doing this extremization let us find first the corresponding equation for the chemical potential. In the RSB case we should calculate the Ξ_{11} element from Eq. (2.18) and substitute it into Eq. (3.10). We use here the so-called one-step replica symmetry breaking (1-RSB) scenario, which is generic for the glass transition in the *p*-spin model [4,5,7], the random energy model [39], and random heteropolymers [15]. Then Parisi's function $\Delta(x)$ is defined by only two parameters:

$$\Delta(x)=\begin{cases}0, & x<x_0,\\ \sigma, & x>x_0.\end{cases} \tag{5.1}$$

The interpretation of σ and the break point x_0 is the following [10]. Within the 1-RSB scenario all replicas are grouped into clusters so that their ultrametric organization has only two levels: the intracluster overlap (or self-overlap) has the strength σ whereas the intercluster overlap is equal to zero. The fraction of replicas that overlap with the strength σ is equal to $1-x_0$. After this simplification the inversion in Eq. (2.18) can be done analytically [see Eq. (AII7) of Ref. [40]]. After a straightforward calculation one gets

$$\Xi_{11}(\mathbf{k};\mu)=\frac{1}{x_0[(a^2/2d)k^2+\mu-2q-2(1-x_0)\sigma]} - \frac{1-x_0}{x_0[(a^2/2d)k^2+\mu-2q-2\sigma]}. \tag{5.2}$$

Insertion of Eq. (5.2) in Eq. (3.10) simply yields

$$\mu-2q_m-2(1-x_0)\sigma_m=O\left(\frac{1}{N}\right), \tag{5.3}$$

where q_m and σ_m are the solutions that extremize the free energies (3.5) and (3.6), respectively. With the 1-RSB assumption [see Eq. (5.1)] the free energy (3.6) becomes

$$f_{\mathrm{RSB}}(\sigma,x_0)=-w_1(1-x_0)\sigma^2+|w_3|(1-x_0)(2-x_0)\sigma^3 -|w_5|(1-x_0)(3-3x_0+x_0^2)\sigma^4. \tag{5.4}$$

It is convenient to represent the chemical potential in the form

$$\mu=\frac{|v|^2}{s(|v|,w)}, \tag{5.5}$$

where $s(|v|,w)$ is a function of $|v|$ and w. For convenience we switch to dimensionless variables (keeping for simplicity the same notations):

$$\frac{v}{a^3}\to v,\quad \frac{w}{a^6}\to w,\quad \frac{z}{a^9}\to z,\quad \frac{s}{a^6}\to s,$$

$$Aa^3\to A,\quad Ba^3\to B,\quad Ca^3\to C. \tag{5.6}$$

We also introduce the reduced values (with overbar)

$$\overline{A}=A|v|,\quad \overline{B}=B|v|^3,\quad \overline{C}=C|v|^5,$$

$$\overline{q}_m=\frac{q_m}{|v|^2},\quad \overline{\sigma}_m=\frac{\sigma_m}{|v|^2},$$

$$\overline{w}_1=w_1|v|,\quad \overline{w}_3=w_3|v|^3,\quad \overline{w}_5=w_5|v|^5. \tag{5.7}$$

After that, Eq. (5.3) for $s(|v|,w)$ (or for the chemical potential) takes the compact form

$$\frac{1}{s}=2\overline{q}_m+2(1-x_0)\overline{\sigma}_m, \tag{5.8}$$

where

$$\overline{q}_m=\frac{-3\overline{B}+\sqrt{(3\overline{B})^2+32|\overline{A}|\overline{C}}}{8\overline{C}}, \tag{5.9}$$

$$\overline{\sigma}_m=\frac{3|\overline{w}_3|(2-x_0)+\sqrt{[3|\overline{w}_3|(2-x_0)]^2-32\overline{w}_1|\overline{w}_5|(3-3x_0+x_0^2)}}{8|\overline{w}_5|(3-3x_0+x_0^2)}, \tag{5.10}$$

$$\overline{w}_1=\overline{A}+2\overline{C}\overline{q}_m^2, \tag{5.11}$$

$$\overline{w}_3=-\overline{B}-4\overline{C}\overline{q}_m, \tag{5.12}$$

$$\overline{w}_5=-\overline{C}, \tag{5.13}$$

and the reduced coefficients read

$$\overline{A}=2-\left(\frac{3}{2\pi}\right)^{3/2}\Gamma\left(\frac{1}{2}\right)s^{1/2},\qquad(5.14)$$

$$\overline{B}=\frac{4}{3}\left[w-\frac{1}{2}\left(\frac{3}{2\pi}\right)^{3/2}\Gamma\left(\frac{3}{2}\right)s^{3/2}\right],\qquad(5.15)$$

$$\overline{C}=2w^2+\frac{2}{3}z|v|-\frac{1}{3}\left(\frac{3}{2\pi}\right)^{3/2}\Gamma\left(\frac{5}{2}\right)s^{5/2}.\qquad(5.16)$$

Equations (5.9) and (5.10) are the results of extremization of Eqs. (4.9) and (5.4), respectively. hroughout the remainder of the paper we will retain the conditions $A<0, B<0, C>0, w_1>0, w_3<0$, and $w_5<0$. This assures that the nontrivial solution σ_m shows up via a first order phase transition, in a similar manner as in *p*-spin spin glasses [4,5] or the random energy model [39]. On the coexistence line between liquid and glassy phases additionally $f_{\mathrm{RSB}}(\sigma_m, x_0)=0$ and this leads to the corresponding equation

$$\frac{\overline{w}_1|\overline{w}_5|}{|\overline{w}_3|^2}=\frac{(2-x_0)^2}{4(3-3x_0+x_0^2)}.\qquad(5.17)$$

The equation for the reduced globule density $c=\rho|v|$ can be easily obtained from Eq. (3.14) under the 1-RSB assumption (5.1). The calculation yields

$$\begin{aligned}c=&4q_m+\frac{4w}{|v|^2}q_m^2+\frac{8}{|v|^3}\left(\frac{w^2}{|v|}+\frac{z}{3}\right)q_m^3-\frac{4w}{|v|^2}\sigma_m^2(1-x_0)\\&+\frac{8}{|v|^3}\left(\frac{w^2}{|v|}+\frac{z}{3}\right)\left[-3q_m\sigma_m^2(1-x_0)+\frac{\sigma_m^3}{2}(1-x_0^2)\right.\\&\left.+\frac{3}{2}\sigma_m^3(1-x_0)^2\right].\end{aligned}\qquad(5.18)$$

Equations (5.8)–(5.16) for the function $s(|v|,w)$ can be solved numerically at given values of the fourth virial coefficient *z* and break point x_0. After substitution of this solution $s(|v|,w)$ in Eq. (5.17) we arrive at the equation for the coexistence line in the plane of $|v|$ and *w*. By changing x_0 one can obtain a whole set of x_0 isolines. We will give the corresponding numerical solution in Sec. V C but first we analyze the validity of the MF approximation given above.

B. Role of fluctuations in RS sector

As mentioned above, the MF solution is valid when the fluctuations are negligible. Generally speaking, this should be required for the RS and RSB sectors of the replica space. In the present paper it is not our intention to consider fluctuations in the RSB sector, which is a rather involved problem that leave for a future publication.

In the RS sector spatial fluctuations are described by the correlation function (C21) (see Appendix C). It is easy to calculate from Eq. (C21) the radial distribution function $g(\mathbf{r})=4\pi r^2\langle\Delta q(\mathbf{r})\Delta q(0)\rangle$ at $d=3$. Again we turn to the reduced variables (5.5)–(5.7). After the inverse Fourier transformation of Eq. (C21), the radial distribution function reads

$$g(\mathbf{r})=\frac{r}{2\overline{X}}\exp\left\{-3|v|\sqrt{\frac{\overline{X}}{\overline{Y}}}\,r\right\},\qquad(5.19)$$

where

$$\overline{X}=\overline{A}+3\overline{q}_m\overline{B}+6\overline{q}_m^2\overline{C}\qquad(5.20)$$

and

$$\overline{Y}=\frac{1}{24\pi}\left(\frac{3}{2}\right)^{3/2}\left[s^{3/2}+5\overline{q}_m s^{5/2}+\frac{63}{4}\overline{q}_m^2 s^{7/2}\right].\qquad(5.21)$$

It is important to note here once more that the quantities $\overline{X}$ and $\overline{Y}$ do not have any additional $|v|$ dependence.

We estimate now the Ginzburg parameter ε_G, (see, e.g., [41]) as the ratio of $g(\mathbf{r})$ at its maximum to $g_m^2=\overline{q}_m^2|v|^4$. Then for the Ginzburg criterion we have the equation

$$|v|^2=\frac{1}{6e\varepsilon_G\overline{q}_m^2\sqrt{\overline{X}(|v|,w)\overline{Y}(|v|,w)}},\qquad(5.22)$$

where *e* is the Napier number. Equation (5.22) for a reasonably small ε_G represents a line in the $(|v|,w)$ plane that separates fluctuating and MF regimes. From now on we will call these two regimes the *liquid* globule and the *glassy* globule, respectively.

From Eq. (5.19) the correlation length is given by

$$\xi=\frac{1}{3|v|}\sqrt{\frac{\overline{X}}{\overline{Y}}}\propto\tau^{-1},\qquad(5.23)$$

which is qualitatively in line with the standard result [27,30,37] and the correct scaling.

From the Gaussian approximation for the effective Hamiltonian in the RS case [Eq. (C18)] it is easy to calculate the corresponding RS free energy, which takes the form

$$\begin{aligned}f_{\mathrm{RS}}\{\overline{q}_m\}=&|v|^3[\overline{A}\overline{q}_m^2+\overline{B}\overline{q}_m^3+\overline{C}\overline{q}_m^4]\\&+\frac{T}{2}\int\frac{d^3\kappa}{(2\pi)^3}\ln[|v|^2\overline{X}+\kappa^2\overline{Y}].\end{aligned}\qquad(5.24)$$

The last integral in Eq. (5.24) diverges at large $\boldsymbol{\kappa}$. This ultraviolet divergence is of no significance as long as the $|v|$ -dependence is the only one we are interested in. For the second derivative of the integral in Eq. (5.24) with respect to $|v|^2$ one has

$$I''_{|v|^2}=-\frac{T\overline{X}^2}{4\pi^2}\int_0^\infty\frac{\kappa^2d\kappa}{[|v|^2\overline{X}+\kappa^2\overline{Y}]^2}=-\frac{T}{16\pi}\left(\frac{\overline{X}}{\overline{Y}}\right)^{3/2}\frac{1}{|v|}.\qquad(5.25)$$

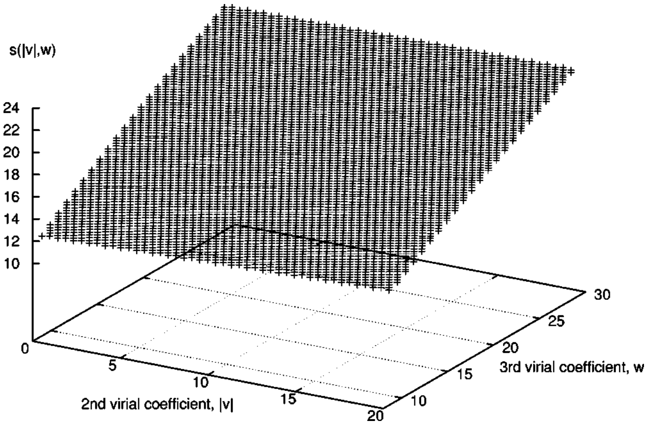

FIG. 1. The dependence of the parameter s [see Eq. (5.5)] on the dimensionless [see Eq. (5.6)] virial coefficients at $z=9$ and $x_0=0.88$.

After that the expression for the RS free energy takes the form

$$f_{\mathrm{RS}}=|v|^3[\overline{Aq_m^2}+\overline{Bq_m^3}+\overline{Cq_m^4}]-\frac{T}{12\pi}\left(\frac{\overline{X}}{\overline{\overline{Y}}}\right)^{3/2}|v|^3. \tag{5.26}$$

We ascribe this branch of the free energy to the liquid globule state and will consider it in more detail in the next subsection.

C. Numerical calculations: Chemical potential, phase diagram, and configurational entropy

Finally we are going to compute the phase diagram for the polymer globule. We recall here that the first step carried out earlier in this paper, i.e., the RS solution, corresponds to the classical coil-globule transition. Here we are now in the position to calculate from the 1-RSB free energy the transition to the glassy state. The numerical solution of Eqs. (5.8)–(5.16) at $z=9$ and $x_0=0.88$ is shown in Fig. 1. As can be seen the function $s(|v|,w)$ depends linearly on w and almost does not depend from $|v|$. This is in agreement with the well-known result [30,37] $\mu\propto|v|^2/w$ [see Eq. (5.5)]. We have also calculated $s(|v|,w)$ at $x_0=0.90, x_0=0.92$, and $x_0=0.95$ and have used these results as input in Eq. (5.17). This eventually leads to x_0 isolines in the glassy globule phase which are plotted in Fig. 2.

The line that is associated with Eq. (5.22) corresponds to the Ginzburg criterion for fluctuations in the RS sector and separates the glassy globule from the liquid one. Obviously, the position of this line depends on the value of $\varepsilon_G \ll 1$ and should be better seen as a crossover from the fluctuating to the mean-field regime. In Fig. 2 this line is given at $\varepsilon_G=0.033$. We have not shown more x_0 isolines explicitly, but it is important to recall that by changing x_0 continuously one can span the whole phase diagram from left to right. It is interesting that the x_0 isolines in Fig. 2 are almost vertical. This means that in a real experiment (upon changing the solvent quality $|v|$ by temperature) always some particular value of x_0 is hit in the glassy phase and stays with it as $|v|$ increases. We recall that $1-x_0$ is the fraction of replicas that overlap with the strength $\sigma_m=\overline{\sigma_m}|v|^2$.

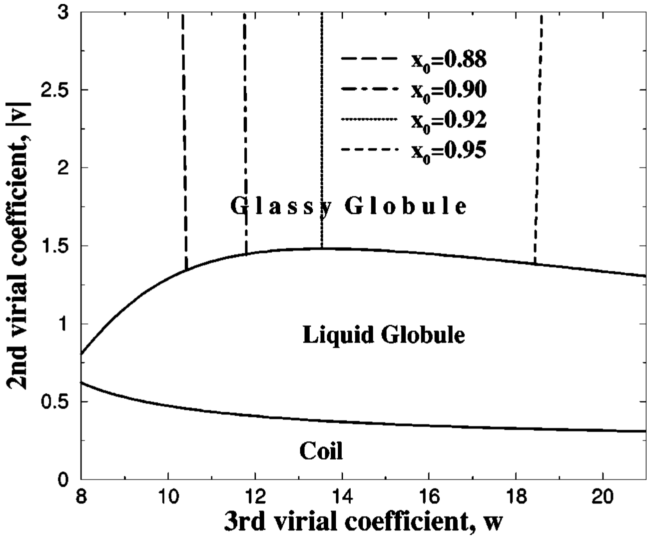

FIG. 2. The phase diagram of the polymer globule in terms of dimensionless virial coefficients. The lower solid line corresponds to the coil-liquid globule second order transition, whereas the upper solid line is associated with the first order liquid-to-solid globule transition. Dotted and dashed x_0 isolines correspond to glassy state with different values of x_0. The other x_0 isolines, which are not shown here, have intermediate values of x_0.

The fact that on the transition line the value of x_0 is less than 1 shows that the transition is thermodynamically of the first order. This is contrary to p-spin spin glasses [4,5,7] and random heteropolymers [13]. It is well known that in these cases the transition has no latent heat (i.e., it is thermodynamically of second order) since $x_0=1$ at the transition point, while the order parameter σ undergoes a jump (i.e., displays a first order transition). In our case the transition is of first order thermodynamically as well as with respect to the order parameter. In Fig. 2 we have shown also the line that corresponds to the coil-globule second order transition [see Eq. (4.16)] at the chain length $N=250$. The critical value $|v|_{\mathrm{cr}}$ on this line is scaled as $1/\sqrt{N}$.

Figure 3 shows the reduced density behavior [see Eq.

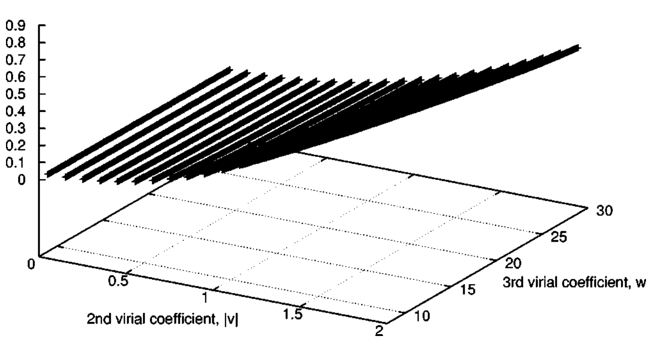

FIG. 3. The reduced density c as a function of virial coefficients at $z=9$ and $x_0 = 0.88$.

(5.18)] at $x_0 = 0.88$ in the same intervals of $|v|$ and w as in Fig. 2. It can be seen that the density on the transition line is fairly small, justifying the use of the virial expansion.

Let us now calculate the configurational entropy $S_{\rm conf}$ (or the complexity) [42], which is usually of interest for glass-forming liquids. The configurational entropy in the liquid globule state can be defined as the difference

$$S_{\rm conf} = S_{\rm liquid} - S_{\rm valley}, \tag{5.27}$$

where

$$S_{\rm liquid} = -\frac{\partial f_{\rm RS}}{\partial T} \tag{5.28}$$

and $S_{\rm valley}$ is the entropy (per particle) that corresponds to one pure state or a valley in the free energy landscape. In order to estimate $S_{\rm valley}$ let us recall from Ref. [43] that the order parameter σ describes the structure of the space of valleys through the probability $P(\sigma)$ that two valleys drawn with the Boltzmann distribution have an overlap σ. For the 1-RSB scenario this function has a rather simple form: $P(\sigma) = x_0\delta(\sigma) + (1-x_0)\delta(\sigma-\sigma_m)$. The dimension of the matrix Δ_{ab}, which within 1-RSB is parametrized by $n(x_0 - 1)/2$ parameters σ, becomes negative at $n \to 0$ and $0 \leqslant x_0 \leqslant 1$. Therefore the free energy $f_{\rm RSB}$ [see Eq. (5.4)] becomes negative, and the factor $-(1-x_0)$ in Eq. (5.4) can be treated as the ''fraction of valleys'' with overlap σ_m. In this case the intravalley free energy can be obtain by dividing out a common factor of $-(1-x_0)$ in Eq. (5.4): $f_{\rm valley} = -f_{\rm RSB}/(1-x_0)$. Then we can estimate $S_{\rm valley}$ in the following way:

$$S_{\rm valley} = \frac{1}{1-x_0}\,\frac{\partial f_{\rm RSB}}{\partial T}. \tag{5.29}$$

The configurational entropy in the glassy globule state is given in the same way as in the p-spin spin glasses [4,43]:

$$S_{\rm conf} = \frac{1}{N}\,[\psi(1) - \psi(1-x_0)], \tag{5.30}$$

where $\psi(x)$ is the digamma function.

By cooling the system along the x_0 isoline at $x_0 = 0.88$, we calculated the configurational entropy for liquid [see Eqs. (5.27)–(5.29)] and glassy [Eq. (5.30)] globules. Figure 4 gives the result of this calculation. As discussed above the transition is of first order, i.e., $S_{\rm conf}$ undergoes a jump which is qualitatively in line with molecular dynamics [22,23] and Monte Carlo [26] simulations. We must bear in mind that the transition temperature in Fig. 4 is also defined by the Ginzburg criterion for fluctuations (see the intersection point of the upper solid line and the $x_0 = 0.88$ isoline in Fig. 2), so that this transition can be treated as a crossover from the fluctuating regime to mean field, where only a few states dominate. This possibility is shown in Fig. 4 by the dashed lines. On the other hand, this behavior is quite different from that of low molecular weight systems or polymer melts where $S_{\rm conf}$ goes to zero continuously as soon as $T \to T_{\rm K}$.

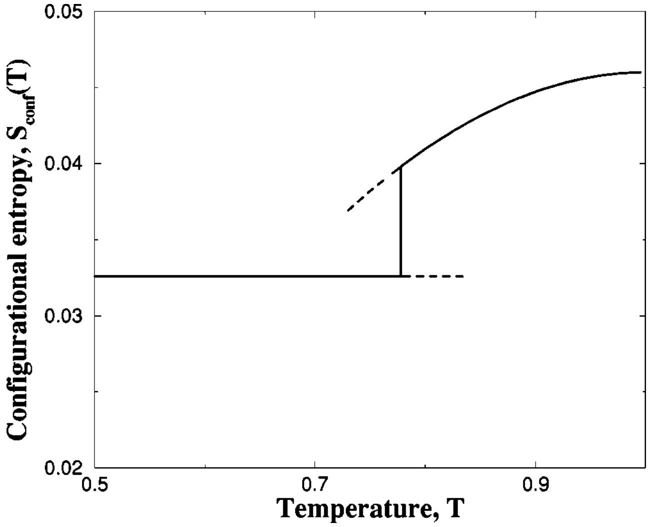

FIG. 4. The configurational entropy $S_{\rm conf}(T)$ as a function of temperature while the globule is cooling from the liquid to the glassy state. For convenience we use dimensionless variables $T/\Theta \to T$ and $S_{\rm conf}/k_{\rm B} \to S_{\rm conf}$, where Θ is the Θ temperature and $k_{\rm B}$ is the Boltzmann constant.

VI. CONCLUSION AND OUTLOOK

We have shown that the homopolymer globule problem can be formulated within the $n \to 0$ limit of free n-component ψ_a^4, ψ_b^6 field theory and can then be mapped onto a disordered one-component model with non-Gaussian random noise. It is of interest that the statistical moments of this noise can be expressed only through the virial coefficients of the pure model, a fact which gives grounds to discuss self-generated disorder. On the other hand, the $n \to 0$ limit is responsible at the same time both for the polymer conformations and for the nontrivial structure of the replica space. Physically this means that units with competitive interactions and constrained by the connectivity possess good preconditions for glass formation.

The Legendre transformation from the pair fields $\psi_a(\mathbf{r})\psi_b(\mathbf{r})$ to the Parisi overlap parameters $Q_{ab}(\mathbf{r})$ leads to an effective Hamiltonian that is akin to corresponding expressions for spin glass models. We have investigated this resulting replicated model within a mean-field Landau-type treatment. First of all, the RS solution of the corresponding equation is associated with the conventional coil-liquid globule transition whereas the RSB solution deeper in the globule state is related to the glassy regime. This mean-field glassy globule phase can be assured only if the fluctuations in RS and RSB sectors are small. In this paper we have studied the fluctuations only in the RS sector and have sketched the corresponding Ginzburg criterion line on the phase diagram. We have calculated the configurational entropy for the liquid and glassy globules and shown that the transition between them is a first order one, as it is also in molecular dynamics and Monte Carlo computer simulations [22,23,26], whereas for the random heteropolymer [13] the freezing is thermodynamically a second order transition. On the other hand, computer simulation [24] and experiment [25] show that the folding in proteins has a latent heat, i.e., the random heteropolymer is a poor model of protein-folding thermodynamics. It has been shown [15,44] that in heteropolymer models where some sequences of monomers have especially low energy in their native conformation the folding is thermodynamically a first order transition.

However, our calculations show that for the homopolymer globule glassy phases occur already deeper in the poor solvent regime. The reasons can be found in competing interactions (virial coefficients of different signs) and the connectivity. A transition with latent heat is possible. In this respect reworking of the random heteropolymer problem within our field-theoretical approach (as oppose to the density functional method [13–15]) would be very interesting. This could elucidate the problem of how the self-generated disorder interplays with quenched disorder and eventually modifies the freezing conditions. It is interesting to note also that some nonpolymer systems without quenched disorder can show glassy behavior as a result of competing interactions on different length scales. As an example one can refer to the frustration-limited domain theory of structural glasses [45] as well as to the ‘‘stripe glasses’’ in doped Mott insulators [46].

The dynamical aspects of the thermodynamic transition discussed above are a matter of crucial importance. The first and foremost question that should be investigated is related to the formation of entropic droplets [4,47] in the RSB sector of the replica space.

ACKNOWLEDGMENT

V.G.R. gratefully acknowledges support by the Sonderforschungsbereich SFB 262 of the Deutsche Forschungsgemeinschaft.

APPENDIX A: FIELD-THEORETICAL REPRESENTATION FOR A GENERAL SELF-INTERACTING CHAIN

Let us represent the Hamiltonian of the self-interacting chain in the form

$$H[\mathbf{r}(s)]=\frac{d}{2a^2}\int_0^N ds\left(\frac{\partial\mathbf{r}}{\partial s}\right)^2+\sum_{m=1}^{\infty}\frac{v_{m+1}}{(m+1)!}\times\int_0^N ds_0 ds_1\cdots ds_m\prod_{i=1}^{m}\delta(\mathbf{r}(s_0)-\mathbf{r}(s_i)),\tag{A1}$$

where v_{m+1} denote the virial coefficients. It is convenient to introduce the density

$$\rho(\mathbf{r})=\int_0^N ds\,\delta(\mathbf{r}-\mathbf{r}(s)).\tag{A2}$$

Then the partition function of the polymer chain

$$Z=\int D\mathbf{r}(s)\exp\{-H[\mathbf{r}(s)]\}\tag{A3}$$

takes the form

$$Z=\int D\mathbf{r}(s)D\rho(\mathbf{r})\,\delta\left[\rho(\mathbf{r})-\int_0^N ds\,\delta(\mathbf{r}-\mathbf{r}(s))\right]\times\exp\left\{-\frac{d}{2a^2}\int_0^N ds\left(\frac{\partial\mathbf{r}}{\partial s}\right)^2-\sum_{m=1}^{\infty}\frac{v_{m+1}}{(m+1)!}\int d^dr\,\rho^{m+1}(\mathbf{r})\right\}.\tag{A4}$$

By making use of the integral representation for the δ function Eq. (A4) can be recast in the form

$$Z=\int D\mathbf{r}(s)D\phi(\mathbf{r})D\rho(\mathbf{r})\exp\left\{i\int d^dr\,\phi(\mathbf{r})\rho(\mathbf{r})-\sum_{m=1}^{\infty}\frac{v_{m+1}}{(m+1)!}\int d^dr\,\rho^{m+1}(\mathbf{r})\right\}\times\int d^drd^dr'\,G(\mathbf{r},\mathbf{r}';[\phi];N),\tag{A5}$$

where

$$G(\mathbf{r},\mathbf{r}';[\phi];N)=\int_{\mathbf{r}(0)=\mathbf{r}}^{\mathbf{r}(N)=\mathbf{r}'}D\mathbf{r}(s)\exp\left\{-\frac{d}{2a^2}\int_0^N ds\left(\frac{\partial\mathbf{r}}{\partial s}\right)^2-i\int_0^N ds\,\phi(\mathbf{r}(s))\right\}.\tag{A6}$$

The corresponding equation for G reads

$$\left[\frac{\partial}{\partial N}-\frac{a^2}{2d}\nabla^2+i\phi(\mathbf{r})\right]G(\mathbf{r},\mathbf{r}';[\phi];N)=\delta(\mathbf{r}-\mathbf{r}')\,\delta(N).\tag{A7}$$

It is convenient to make the Laplace transformation

$$G(\mathbf{r},\mathbf{r}';[\phi];\mu)=\int_0^{\infty}dN\,G(\mathbf{r},\mathbf{r}';[\phi];N)\exp(-\mu N),\tag{A8}$$

after which the equation for $G(\mathbf{r},\mathbf{r}';[\phi];\mu)$ yields

$$G(\mathbf{r},\mathbf{r}';[\phi];\mu)=\frac{\int D\psi\psi(\mathbf{r})\psi(\mathbf{r}')\exp\left\{-\frac{1}{2}\int d^dr\,\psi(\mathbf{r})[\mu-(a^2/2d)\nabla^2+i\phi(\mathbf{r})]\psi(\mathbf{r}')\right\}}{\int D\psi\exp\left\{-\frac{1}{2}\int d^dr\,\psi(\mathbf{r})[\mu-(a^2/2d)\nabla^2+i\phi(\mathbf{r})]\psi(\mathbf{r}')\right\}}. \tag{A9}$$

In order to avoid the denominator in Eq. (A9) we should upgrade the field ψ by introducing the n-component field $\vec{\psi}=\{\psi_1,\psi_2,\ldots,\psi_n\}$. Then by using the replica trick we have

$$G(\mathbf{r},\mathbf{r}';[\phi];\mu)=\lim_{n\to 0}\int\prod_{a=1}^{n}D\psi_\alpha\psi_1(\mathbf{r})\psi_1(\mathbf{r}')\times\exp\left\{-\frac{1}{2}\sum_{a=1}^{n}\int d^dr\,\psi_a(\mathbf{r})\times\left[\mu-\frac{a^2}{2d}\nabla^2+i\phi(\mathbf{r})\right]\psi_a(\mathbf{r}')\right\}. \tag{A10}$$

One can now make the Laplace transformation of aboth sides of Eq. (A5) and substitute it in Eq. (A10). Integration first over the field $\phi(\mathbf{r})$ and then over $\rho(\mathbf{r})$ results in the following expression for the grand canonical partition function of a polymer chain with ends fixed at points $\mathbf{r}$ and $\mathbf{r}'$:

$$\Xi(\mathbf{r},\mathbf{r}';\mu)=\lim_{n\to 0}\int\prod_{a=1}^{n}D\psi_a\psi_1(\mathbf{r})\psi_1(\mathbf{r}')\exp\{-H_n[\vec{\psi};\mu]\}, \tag{A11}$$

where

$$H_n[\vec{\psi};\mu]=\frac{1}{2}\int d^dr\sum_{a=1}^{n}\psi_a(\mathbf{r})\left[\mu-\frac{a^2}{2d}\nabla^2\right]\psi_a(\mathbf{r}')+\sum_{m=1}^{\infty}\frac{v_{m+1}}{(m+1)!}\int d^dr\sum_{a=1}^{n}\left[\frac{1}{2}\psi_a^2(\mathbf{r})\right]^{m+1}. \tag{A12}$$

APPENDIX B: THE CONNECTION TO A RANDOM MODEL

Here we prove that in a poor solvent the polymer problem [see Eqs. (2.3) and (2.4)] can be connected to a one-component random model. We shall restrict our consideration to the second and third virial coefficients. The generalization to the case with an arbitrary number of virial coefficients is straightforward.

Let us consider the one-component random model with Hamiltonian

$$\mathcal{H}\{\psi\}=\frac{1}{2}\int d^dr\left[\mu\psi^2(\mathbf{r})+\frac{a^2}{2d}(\nabla\psi)^2+t(\mathbf{r})\psi^2(\mathbf{r})\right], \tag{B1}$$

where $t(\mathbf{r})$ is a non-Gaussian random field with the generating functional

$$\Phi\{\rho(\mathbf{r})\}\equiv\int Dt(\mathbf{r})P\{t(\mathbf{r})\}\exp\left\{-\int d^drt(\mathbf{r})\rho(\mathbf{r})\right\}=\exp\left\{\frac{|v|}{8}\int d^dr\,\rho^2(\mathbf{r})-\frac{w}{3!8}\int d^dr\,\rho^3(\mathbf{r})\right\}. \tag{B2}$$

In Eq. (B2) $P\{t(\mathbf{r})\}$ is the distribution functional of the field $t(\mathbf{r})$. One can easily check that the replication of the Hamiltonian (B1) and the subsequent averaging over $t(\mathbf{r})$, i.e.,

$$\overline{Z^n}=\overline{\int\prod_{a=1}^{n}D\psi_a\exp\left\{-\sum_{a=1}^{n}\mathcal{H}\{\psi_a\}\right\}}, \tag{B3}$$

leads to the effective replicated Hamiltonian (2.4).

From the probabilistic interpretation (B2) one can explicitly find the central moments of $t(\mathbf{r})$. The expansion of both sides of Eq. (B2) yields

$$\sum_{m=0}^{\infty}\frac{(-1)^m}{m!}\int dr_1\cdots dr_m\overline{t(r_1)t(r_2)\cdots t(r_m)}\rho(r_1)\rho(r_2)\cdots\rho(r_m)=\sum_{k=0}^{\infty}\frac{1}{k!}\sum_{l=0}^{k}\frac{k!(-1)^l}{l!(k-l)!}\left[\frac{|v|}{8}\int d^dr\rho^2(\mathbf{r})\right]^{k-l}\left[\frac{w}{3!8}\int d^dr\rho^3(\mathbf{r})\right]^l. \tag{B4}$$

By making the m terms of $\rho(\mathbf{r})$ on both sides of Eq. (B4) equal, one gets

$$\int dr_1\cdots dr_m\overline{t(r_1)t(r_2)\cdots t(r_m)}\rho(r_1)\rho(r_2)\cdots\rho(r_m)=\sum_{k=\{m/3\}}^{[m/2]}\frac{m!}{(m-2k)!(3k-m)!}\times\left[\frac{|v|}{8}\int d^dr\rho^2(\mathbf{r})\right]^{3k-m}\left[\frac{w}{3!8}\int d^dr\rho^3(\mathbf{r})\right]^{m-2k}, \tag{B5}$$

where $[m/2]$ stands for the greatest integer number less than $m/2$ and $\{m/3\}$ is the smallest integer number larger than $m/3$. By making use of the representations $\int d^dr\rho^2(\mathbf{r})=\int d^dr_1d^dr_2\delta(\mathbf{r}_1-\mathbf{r}_2)\rho(\mathbf{r}_1)\rho(\mathbf{r}_2)$ and $\int d^dr\rho^3(\mathbf{r})=\int d^dr_3d^dr_4d^dr_5\delta(\mathbf{r}_5-\mathbf{r}_4)\delta(\mathbf{r}_5-\mathbf{r}_3)\rho(\mathbf{r}_3)\rho(\mathbf{r}_4)\rho(\mathbf{r}_5)$ one finally gets

$$\overline{t(r_1)t(r_2)\cdots t(r_m)}=\sum_{k=\{m/3\}}^{[m/2]}\frac{m!}{(m-2k)!(3k-m)!}\left(\frac{|v|}{8}\right)^{3k-m}\left(\frac{w}{3!8}\right)^{m-2k}\delta(\mathbf{r}_1-\mathbf{r}_2)\delta(\mathbf{r}_3-\mathbf{r}_4)\cdots\delta(\mathbf{r}_{6k-2m-1}-\mathbf{r}_{6k-2m})\times\delta(\mathbf{r}_{6k-2m+1}-\mathbf{r}_{6k-2m+2})\delta(\mathbf{r}_{6k-2m+1}-\mathbf{r}_{6k-2m+3})\cdots\delta(\mathbf{r}_{m-2}-\mathbf{r}_{m-1})\delta(\mathbf{r}_{m-2}-\mathbf{r}_m). \tag{B6}$$

In Eq. (B6) the second line includes $3k-m$ δ functions with arguments successively pairwise divided between $6k-2m$ points. The third line includes $m-2k$ δ functions so that in each successive pair of them one $\mathbf{r}$ point is common.

Let us consider some particular cases of Eq. (B6).

(i) $m=1$. Then $\{m/3\}=1$, $[m/2]=0$, and

$$\overline{t(\mathbf{r})}=0. \tag{B7}$$

(ii) $m=2$. Then $\{m/3\}=1$, $[m/2]=1$, and Eq. (B6) reads

$$\overline{t(\mathbf{r}_1)t(\mathbf{r}_2)=\frac{|v|}{4}}\delta(\mathbf{r}_1-\mathbf{r}_2). \tag{B8}$$

(iii) At $m=3$,$\{m/3\}=1$, $[m/2]=1$ (i.e., $k=1$), and one gets

$$\overline{t(\mathbf{r}_1)t(\mathbf{r}_2)t(\mathbf{r}_3)}=\frac{w}{8}\delta(\mathbf{r}_1-\mathbf{r}_2)\delta(\mathbf{r}_1-\mathbf{r}_3). \tag{B9}$$

(iv) At $m=4$,$\{m/3\}=2$, $[m/2]=2$ (i.e., $k=2$), and

$$\overline{t(\mathbf{r}_1)t(\mathbf{r}_2)t(\mathbf{r}_3)t(\mathbf{r}_4)}=\frac{3}{16}|v|^2\delta(\mathbf{r}_1-\mathbf{r}_2)\delta(\mathbf{r}_3-\mathbf{r}_4). \tag{B10}$$

(v) Finally at $m=5$,$\{m/3\}=2$,$[m/2]=2$, and

$$\overline{t(\mathbf{r}_1)t(\mathbf{r}_2)t(\mathbf{r}_3)t(\mathbf{r}_4)t(\mathbf{r}_5)}=\frac{5!}{3!64}|v|w\delta(\mathbf{r}_1-\mathbf{r}_2)\times\delta(\mathbf{r}_3-\mathbf{r}_4)\delta(\mathbf{r}_3-\mathbf{r}_5). \tag{B11}$$

The important feature of these moments is that all of them are positive, which means that $t(\mathbf{r})$ is real.

APPENDIX C: SPATIAL FLUCTUATIONS FOR A WEAKLY INHOMOGENEOUS GLOBULE

In this Appendix we give the Landau expansion only for the case when q and the coefficients $\Gamma^{(2)},\Gamma^{(3)},\Gamma^{(4)}$ are weakly $\mathbf{k}$ dependent in the RS sector. The spatial Fourier transformation in Eq. (3.1) leads to the following effective Hamiltonian:

$$H_{\mathrm{RS}}\{q(\mathbf{k})\}=\int\frac{d^dk}{(2\pi)^d}\Gamma^{(2)}(\mathbf{k})q(\mathbf{k})q(-\mathbf{k})+\int\frac{d^dk_1d^dk_2}{(2\pi)^2d}\Gamma^{(3)}(\mathbf{k}_1,\mathbf{k}_2)q(\mathbf{k}_1)q(\mathbf{k}_2)\times q(-\mathbf{k}_1-\mathbf{k}_2)+\int\frac{d^dk_1d^dk_2d^dk_3}{(2\pi)^3d}\times\Gamma^{(4)}(\mathbf{k}_1,\mathbf{k}_2,\mathbf{k}_3)q(\mathbf{k}_1)q(\mathbf{k}_2)q(\mathbf{k}_3)\times q(-\mathbf{k}_1-\mathbf{k}_2-\mathbf{k}_3)+\cdots, \tag{C1}$$

where

$$\Gamma^{(2)}(\mathbf{k})=\frac{2}{|v|}-\int\frac{d^d\kappa}{(2\pi)^d}\frac{1}{[(a^2/2d)\kappa^2+\mu][(a^2/2d)(\kappa-\mathbf{k})^2+\mu]}, \tag{C2}$$

$$\Gamma^{(3)}(\mathbf{k}_1,\mathbf{k}_2)=\frac{4}{3}\left[\frac{w}{|v|^3}-\int\frac{d^d\kappa}{(2\pi)^d}\frac{1}{[(a^2/2d)\kappa^2+\mu][(a^2/2d)(\kappa-\mathbf{k}_1)^2+\mu][(a^2/2d)(\kappa-\mathbf{k}_1-\mathbf{k}_2)^2+\mu]}\right], \tag{C3}$$

$$\Gamma^{(4)}(\mathbf{k}_1,\mathbf{k}_2,\mathbf{k}_3)=\frac{2}{|v|^4}\left(\frac{w^2}{|v|}+\frac{z}{3}\right)-2\int\frac{d^d\kappa}{(2\pi)^d}$$
$$\times\frac{1}{[(a^2/2d)\kappa^2+\mu][(a^2/2d)(\kappa-\mathbf{k}_1)^2+\mu][(a^2/2d)(\kappa-\mathbf{k}_1-\mathbf{k}_2)^2+\mu][(a^2/2d)(\kappa-\mathbf{k}_1-\mathbf{k}_2-\mathbf{k}_3)^2+\mu]}. \tag{C4}$$

For weak fluctuations around the MF solution q_m to be investigated one should estimate the Hessian

$$\left.\frac{\delta^2 H_{\mathrm{RS}}}{\delta q(\mathbf{r}_1)\,\delta q(\mathbf{r}_2)}\right|_{q=q_m}=2\Gamma^{(2)}(\mathbf{r}_1-\mathbf{r}_2)+6q_m \times\int d^d r_3\Gamma^{(3)}(\mathbf{r}_2-\mathbf{r}_1,\mathbf{r}_3-\mathbf{r}_1) +12q_m^2\int d^d r_3 d^d r_4\Gamma^{(4)}(\mathbf{r}_2-\mathbf{r}_1,\mathbf{r}_3 -\mathbf{r}_1,\mathbf{r}_4-\mathbf{r}_1)+\cdots, \tag{C5}$$

or, in the Fourier space,

$$\left.\frac{\delta^2 H_{\mathrm{RS}}}{\delta q(\mathbf{k})\,\delta q(-\mathbf{k})}\right|_{q=q_m}=2\Gamma^{(2)}(\mathbf{k})+6q_m\Gamma^{(3)}(\mathbf{k},\mathbf{k}=\mathbf{0}) +12q_m^2\Gamma^{(4)}(\mathbf{k},\mathbf{k}=\mathbf{0},\mathbf{k}=\mathbf{0})+\cdots. \tag{C6}$$

The resulting effective Hamiltonian expansion around the MF solution takes the form

$$\begin{aligned}H_{\mathrm{RS}}\{q_m,\Delta q(\mathbf{k})\}&=H_{\mathrm{RS}}\{q_m\}+\frac{1}{2}\int\frac{d^dk}{(2\pi)^d}\times\left.\frac{\delta^2 H_{\mathrm{RS}}}{\delta q(\mathbf{k})\,\delta q(-\mathbf{k})}\right|_{q=q_m}\Delta q(\mathbf{k})\Delta q(-\mathbf{k})\\&=Aq_m^2+Bq_m^3+Cq_m^4\\&\quad+\int\frac{d^dk}{(2\pi)^d}[\Gamma^{(2)}(\mathbf{k})+3q_m\Gamma^{(3)}(\mathbf{k},\mathbf{k}=\mathbf{0})\\&\quad+6q_m^2\Gamma^{(4)}(\mathbf{k},\mathbf{k}=\mathbf{0},\mathbf{k}=\mathbf{0})]\Delta q(\mathbf{k})\\&\quad\times\Delta q(-\mathbf{k}),\end{aligned} \tag{C7}$$

where

$$\Delta q(\mathbf{k})=q(\mathbf{k})-q_m \tag{C8}$$

and

$$A=\Gamma^{(2)}(0),\quad B=\Gamma^{(3)}(0,0),\quad C=\Gamma^{(4)}(0,0,0), \tag{C9}$$

or

$$A=\frac{2}{|v|}-\left(\frac{d}{2\pi a^2}\right)^{d/2}\frac{\Gamma((4-d/2))}{\mu^{(4-d/2)}} \tag{C10}$$

$$B=\frac{4}{3}\left[\frac{w}{|v|^3}-\left(\frac{d}{2\pi a^2}\right)^{d/2}\frac{\Gamma((6-d/2))}{2\mu^{(6-d)/2}}\right] \tag{C11}$$

$$C=\frac{2}{|v|^4}\left(\frac{w^2}{|v|}+\frac{z}{3}\right)-\left(\frac{d}{2\pi a^2}\right)^{d/2}\frac{\Gamma((8-d/2))}{3\mu^{(8-d/2)}}, \tag{C12}$$

$$w_1=A+3B(q-f)+6C(q-f)^2, \tag{C13}$$

$$w_2=-3Bf-4Cf^4, \tag{C14}$$

$$w_3=-B-4C(q-f), \tag{C15}$$

$$w_4=-4Cf, \tag{C16}$$

$$w_5=-C. \tag{C17}$$

It is easy to estimate the integrand in Eq. (C7) at small $\mathbf{k}$ (weak inhomogeneity). The straightforward calculations yields

$$H_{\mathrm{RS}}\{q_m,\Delta q(\mathbf{k})\}=H_{\mathrm{RS}}\{q_m\}+\int\frac{d^dk}{(2\pi)^d}\ \{X(|v|,w) +(ka)^2Y(|v|,w)\}\Delta q(\mathbf{k})\Delta q(-\mathbf{k}), \tag{C18}$$

where

$$X=A+3q_mB+6q_m^2C \tag{C19}$$

and

$$\begin{aligned}Y=&\left(\frac{1}{2\pi da^2}\right)^{d/2}\ \frac{2d-3}{12\mu^{(6-d)/2}}\ \Gamma\left(\frac{6-d}{2}\right)\\&+q_m\left(\frac{1}{2\pi da^2}\right)^{d/2}\ \frac{3d-4}{9\mu^{(8-d)/2}}\ \Gamma\left(\frac{8-d}{2}\right)\\&+q_m^2\left(\frac{1}{2\pi da^2}\right)^{d/2}\ \frac{4d-5}{20\mu^{(10-d)/2}}\ \Gamma\left(\frac{10-d}{/2}\right).\end{aligned} \tag{C20}$$

From Eq. (C18) it is obvious that the corresponding correlation function

$$\langle|\Delta q(\mathbf{k})|^2\rangle=\frac{1}{X(|v|,w)+(ka)^2Y(|v|,w)}. \tag{C21}$$

[1] W. Götze in *Liquids, Freezing and the Glass Transition*, edited by J.P. Hansen, D. Levesque, and J. Zinn-Justin (North-Holland, Amsterdam, 1991).

[2] J.-P. Bouchard, L.F. Cugliandolo, J. Kurchan and M. Mézard, in *Spin Glasses and Random Fields*, edited by A.P. Young (World Scientific, Singapore, 1998).

[3] W. Kauzmann, Chem. Rev. **43**, 219 (1948); J. H. Gibbs and E.A. DiMarzio, J. Chem. Phys. **28**, 373 (1958).

[4] T.R. Kirkpatrick and P. Wolynes, Phys. Rev. B **36**, 8552 (1987); T.R. Kirkpatrick and D. Thirumalai, *ibid.* **B36**, 5388 (1987); **37**, 5342 (1987).

[5] A. Crisanti and H.-J. Sommers, Z. Phys. **87**, 341 (1992).

[6] S. Kirkpatrick and D. Sherrington, Phys. Rev. B **17**, 4384 (1978).

[7] T.R. Kirkpatrick and D. Thirumalai, Transp. Theory Stat. Phys. **24**, 927 (1995).

[8] J.-P. Bouchard and M. Mézard, J. Phys. I **4**, 1109 (1994); E. Marinari, G. Parisi, and F. Ritort, J. Phys. A **27**, 7615 (1994); G. Migliorini and F. Ritort, *ibid.* **27**, 7669 (1994).

[9] K. Binder and A.P. Young, Rev. Mod. Phys. **58**, 801 (1986).

[10] M. Mézard, G. Parisi, and M.A. Virasoro, *Spin Glass Theory and Beyond* (World Scientific, Singapore, 1986).

[11] V.S. Dotsenko, *The introduction to the Theory of Spin Glasses and Neural Networks* (World Scientific, Singapore, 1994).

[12] T. Garel and H. Orland, Europhys. Lett. **6**, 597 (1988).

[13] E.I. Shakhnovich and A.M. Gutin, Biophys. Chem. **34**, 187 (1989).

[14] C.D. Sfatos, A.M. Gutin, and E.I. Shakhnovich, Phys. Rev. E **48**, 465 (1993).

[15] V.S. Pande, A.Yu. Grosberg, and T. Tanaka, Rev. Mod. Phys. **72**, 259 (2000).

[16] P.G. de Gennes, *Scaling Concepts in Polymer Science* (Cornell University Press, Ithaca, NY, 1976).

[17] A. Milchev and K. Binder, Europhys. Lett. **26**, 671 (1994).

[18] S. Kreitmeier, J. Chem. Phys. **112**, 6925 (2000).

[19] S. Kreitmeier, M. Wittkop, and D. Göritz, Phys. Rev. E **59**, 1982 (1999).

[20] M. Wittkop, S. Kreitmeier, and D. Göritz, J. Chem. Phys. **104**, 3373 (1996).

[21] R. Du, A.Yu. Grosberg. T. Tanaka, and M. Rubinstein, e-print cond-mat/9905105.

[22] Y. Zhou, C.K. Hall, and M. Karplus, Phys. Rev. Lett. **77**, 2822 (1996).

[23] Y. Zhou and M. Karplus, J.M. Wichert, and C.K. Hall, J. Chem. Phys. **107**, 10691 (1997).

[24] Y. Zhou and M. Karplus, Proc. Natl. Acad. Sci. U.S.A. **94**, 14429 (1997).

[25] O.B. Ptitsyn, Adv. Protein Chem. **47**, 83 (1995).

[26] W. Paul and M. Müller, J. Chem. Phys. **115**, 630 (2001).

[27] P.G. de Gennes, Phys. Lett. **36A**, 339 (1972).

[28] T.A. Vilgis, J. Phys. A **24**, 5321 (1991).

[29] P.G. de Gennes, J. Phys. (France) **36**, L55 (1975).

[30] A.L. Kholodenko and K.F. Freed, J. Phys. A **17**, 2703 (1984); J. Chem. Phys. **80**, 900 (1984).

[31] V.J. Emery, Phys. Rev. B **11**, 239 (1975).

[32] D. Jasnow and M. Fisher, Phys. Rev. B **13**, 1112 (1976).

[33] S.V. Panyukov and Y. Rabin, Phys. Rep. **269**, 1 (1996).

[34] T. Ohta and K. Kawasaki, Macromolecules **19**, 2621 (1986).

[35] G. Fredrickson and E. Helfand, J. Chem. Phys. **93**, 2048 (1990).

[36] J. Zinn-Justin, *Quantum Field Theory and Critical Phenomena* (Clarendon Press, Oxford, 1989).

[37] A.Yu. Grosberg and A.R. Khokhlov, *Statistical Physics of Macromolecules* (AIP, Woodbury, NY, 1994).

[38] T.A. Vilgis and P. Haronska, Macromolecules **27**, 6465 (1994).

[39] B. Derrida, Phys. Rev. B **24**, 2613 (1981).

[40] M. Mézard and G. Parisi, J. Phys. I **1**, 809 (1991).

[41] Yu.L. Klimontovich, *Statistical Physics* (Harwood Academic Publishers, New York, 1986).

[42] R.G. Palmer, Adv. Phys. **31**, 669 (1982).

[43] D.J. Gross and M. Mézard, Nucl. Phys. B: Field Theory Stat. Syst. **240**, 431 (1984).

[44] S. Ramanathan and E. Shakhnovich, Phys. Rev. E **50**, 1303 (1994).

[45] D. Kivelson, S.A. Kivelson, X. Zhao, Z. Nussinov, and G. Tarjus, Physica B **219**, 27 (1995).

[46] J. Schmalian and P. Wolynes, Phys. Rev. Lett. **85**, 836 (2000).

[47] S. Takada and P. Wolynes, J. Chem. Phys. **107**, 9585 (1997).